W_6S_8 Inorganic Clusters with Organic TTF Derivative Ligands: in Pursuit of Multidimensional Conductive Networks

Min Yuan, Burak Ülgüt, Michael McGuire, Kazutake Takada, Francis J. DiSalvo,* Stephen Lee,* and Héctor Abruña

Department of Chemistry and Chemical Biology, Baker Laboratory, Cornell University, Ithaca, New York 14853-1301

Received January 3, 2006. Revised Manuscript Received July 11, 2006

A series of new molecular cluster complexes with TTF derivative ligands attached to an inorganic W_6S_8 core were prepared, namely $W_6S_8(PEt_{3-n}TTF_n)_6$ ($n = 1, 2$). By incorporating two useful structural motifs (the well-known $\pi-\pi$ stacking geometry of TTF molecules and the high symmetry of octahedral clusters) into one network structure, we constructed multidimensional networks. Single-crystal X-ray diffraction studies revealed intercluster TTF π-contacts in one and two dimensions, for $W_6S_8(PEt_2TTF)_6$ and $W_6S_8(PEtTTF_2)_6$, respectively. The redox properties of $W_6S_8(PEt_2TTF)_6$ were studied by cyclic voltammetry. Mid- and far-IR and XPS (X-ray photoelectron spectroscopy) characterizations were performed on both the $W_6S_8(PEt_2TTF)_6$ cluster and its oxidized product, which helped to elucidate the identity of the poorly crystalline oxidized product. Four-point contact electrical conductivity measurements were performed on a pressed pellet of the oxidized powder product $W_6S_8(PEt_2TTF)_6{\cdot}xPF_6$ ($x \approx 5$) with $\sigma_{RT} \approx 1 \times 10^{-4}$ S cm^{-1}, whereas the neutral cluster complex is insulating at room temperature.

Introduction

Over the past few decades, intense interest has been drawn to the family of organic metals based on tetrathiafulvalene (TTF) and its derivatives, mainly because of the superconducting behavior discovered in some of these systems.[1−3] Among the numerous systems that have been studied, only a handful of structures demonstrated the desired multidimensional metallic bonding.[4] This article is motivated by a perceived need for new electronically TTF-derived multidimensional crystal topologies.[5]

Metallic TTF systems almost invariably contain one-dimensional stacks of co-facial TTF molecules. Any multidimensionality comes in large part from additional interchain S···S interactions. The formation of such intermolecular S···S contacts is generally impossible to predict. It is therefore desirable to turn to concentrate on the excellent $\pi-\pi$ cofacial TTF contact so ubiquitous in TTF chemistry and then to covalently link the TTF molecules to one another in a way so as to potentially ensure a three-dimensional crystal packing.

To tackle this idea, we prepared clusters of TTF molecules (TTF−π ligands attached to highly symmetrical W_6S_8 inorganic cluster core), a system that bears some structural similarity to the superconducting alkali-metal-doped fulleride family.[6,7] In the fulleride case, the building units are the highly symmetrical spherical shaped fullerene molecules, which form face-centered-cubic (fcc) closest packing; thus, each fullerene is in contact with 12 of its nearest neighbors. Because of the curvature of the molecule, all are in π-contact with one another. The resulting π-bands are three-dimensional. In our design, we wished to exploit building units of high symmetry, i.e., the octahedral W_6S_8 clusters, to construct similar fcc closest-packing structures. With six ligands to promote intercluster $\pi-\pi$ interactions from TTF cofacial stacking, we hoped to create a system whose geometric shape favors orbital interactions in more than one dimension.

Research efforts using group 6 octahedral chalcogenide metal clusters M_6Q_8 (M = Cr,[8−10] Mo,[11−16] W;[17−23] Q = S, Se, Te) as building units for interesting new materials have

* To whom correspondence should be addressed. E-mail: fjd3@cornell.edu (F. J. D.); sl137@cornell.edu (S.L.).

(1) Bechgaard, K.; Jacobsen, C. S.; Mortensen, K.; Pedersen, H. J.; Thorup, N. *Solid State Commun.* **1980**, *33*, 1119−1125.
(2) Jérome, D.; Mazaud, A.; Ribault, M.; Bechgaard, K. *J. Phys. Lett.* **1980**, *41*, 95−98.
(3) Parkin, S. S. P.; Engler, E. M.; Schumaker, R. R.; Lagier, R.; Lee, V. Y.; Scott, J. C.; Greene, R. L. *Phys. Rev. Lett.* **1983**, *50*, 270−273.
(4) This multidimensionality of the band structure is a perceived request for low-temperature metals, which promises an increased likelihood of low-temperature superconductivity. See: (a) Williams, J. M.; Wang, H. H.; Emge, T. J.; Geiser, U.; Beno, M. A.; Leung, P. C. W.; Carlson, K. D.; Thorn, R. J.; Schultz, A. J.; Whangbo, M. H. *Prog. Inorg. Chem.* **1987**, *35*, 51−218. (b) Mori, T. *Bull. Chem. Soc. Jpn.* **1998**, *71*, 2509−2526. (c) Mori, T.; Mori, H.; Tanaka, S. *Bull. Chem. Soc. Jpn.* **1999**, *72*, 179−197. (d) Segura, J. L.; Martín, N. *Angew. Chem., Int. Ed.* **2001**, *40*, 1372−1409.
(5) Bryce, M. R. *J. Mater. Chem.* **1995**, *5*, 1481−1496.
(6) Hebard, A. F.; Rosseinsky, M. J.; Haddon, R. C.; Murphy, D. W.; Glarum, S. H.; Palstra, T. T. M.; Ramirez, A. P.; Kortan, A. R. *Nature* **1991**, *350*, 600−601.
(7) Tanigaki, K.; Ebbesen, T. W.; Saito, S.; Mizuki, J.; Tsai, J. S.; Kubo, Y.; Kuroshima, S. *Nature* **1991**, *352*, 222−223.
(8) Hessen, B.; Siegrist, T.; Palstra, T.; Tanzler, S. M.; Steigerwald, M. L. *Inorg. Chem.* **1993**, *32*, 5165−5169.
(9) Tsuge, K.; Imoto, H.; Saito, T. *Bull. Chem. Soc. Jpn.* **1996**, *69*, 627−636.
(10) Kamiguchi, S.; Imoto, H.; Saito, T.; Chihara, T. *Inorg. Chem.* **1998**, *37*, 6852−6857.
(11) Saito, T.; Yamamoto, N.; Nagase, T.; Tsuboi, T.; Kobayashi, K.; Yamagata, T.; Imoto, H.; Unoura, K. *Inorg. Chem.* **1990**, *29*, 764−770.
(12) Hilsenbeck, S. J.; Young, V. G., Jr.; McCarley, R. E. *Inorg. Chem.* **1994**, *33*, 1822−1832.

10.1021/cm0600071 CCC: $33.50
Published on Web 08/12/2006

continued ever since the breakthrough synthesis of the first molecular octahedral cluster $Mo_6S_8(PEt_3)_6$ in the late 1980s.[24] These clusters have attracted continued attention partly because of their structural relationship with the well-known molybdenum-based superconducting Chevrel phases.[25,26] Because of their high symmetry, these clusters have been used as building blocks to construct interlinked network structures.[14,27] π-Conjugated ditopic ligands have been employed as electronically active linkers to link W_6S_8 clusters in a 3-D fashion in an attempt to produce materials with interesting electronic properties.[28,29] Organic ligands that bind strongly to such inorganic clusters can be either nitrogen- or phosphorus-containing Lewis basic ligands, where the N or P atoms are able to directly attach to the metal atoms on the cluster cores to produce molecular species with reasonable solubility and stability.

Because both the W_6S_8 cluster core and TTF π-ligands can be oxidized at similar potentials,[30,31] we hope to electronically couple the π-systems of the TTF molecules in these clusters to the W_6S_8 cluster core and indirectly couple these π-systems to one another through the inorganic core.

A neutral W_6S_8 cluster has a metal electron count (MEC) of 20[28] and is known to be easily reduced or oxidized. The half-wave potential for the $[W_6S_8]^{0/+1}$ couple lies near 0.15 V (vs SCE).[30] The structure of one oxidized cluster, $[W_6S_8(PEt_3)_6]PF_6$, has been reported.[32] On the other hand, TTF and its derivatives, as good electron donors, can also be oxidized at relatively low potentials (0.30 V for first oxidation vs SCE).[31] Therefore, it is experimentally conceivable that simultaneous oxidation of both the inorganic cluster core and TTF derivative ligands can be achieved. Such oxidation may lead to metallic conductivity through TTF $\pi-\pi$ contacts between and through highly symmetrical W_6S_8 units and would provide us with not only a fascinating structural motif, but also a potential electronically multidimensional system.

Here, we report the synthesis and structural studies of a series of $W_6S_8(PEt_{3-n}TTF_n)_6$ ($n = 1, 2$) complexes. The experimentally observed intercluster TTF $\pi-\pi$ contacts present in these structures in one or two dimensions suggest that the strategy of organizing the TTF into orthogonal directions may be generally useful in producing nearly isotropic conductivity.

Experimental Section

General. $W_6S_8(4\text{-tbp})_6$ (4-tbp = 4-*tert*-butylpyridine) was synthesized according to previously reported procedures[21] and used as a precursor cluster for ligand-exchange reactions. The ligands tetrathiafulvalene diethylphosphine and bis(tetrathiafulvalene)-ethylphosphine were synthesized on the basis of procedures developed by Batail's group[33] with some modifications. Tetrathiafulvalene from TCI America and all other reagents from Aldrich were used without further purification. Diethyl ether and benzene were treated with sodium wire and distilled under reduced pressure. All reactants and solvents were stored either under nitrogen or in a glovebox filled with argon. All glassware was oven-dried before use. All the operations were carried out under an inert gas atmosphere (in the glovebox or in a Schlenk line with argon protection) unless otherwise stated.

^{1}H NMR spectra were obtained on a Varian Mercury-300 spectrometer with no ^{31}P decoupling and were referenced to an internal residual solvent peak. ^{31}P NMR spectra were collected on the same spectrometer at 162 MHz with 85% H_3PO_4 as an external standard and with ^{1}H decoupling. Powder X-ray diffraction was done on an INEL MPD diffractomer (XRG 3000, CPS 120 detector) at 25 mA and 35 kV for Cu Kα_1 ($\lambda = 1.54056$ Å), with a silver behenate and elemental silicon standard. Elemental analysis was done by Robertson Microlit Laboratories, Madison, NJ.

Synthesis of TTF Phosphine Ligands PEt_2TTF and $PEtTTF_2$. Our preparation is based on the preparation reported by Batail et al.[33] which has been modified as described below. To a solution of TTF (0.51 g, 2.5 mmol) in freshly distilled diethyl ether (50 mL) at −78 °C was added 1.0 equiv of LDA, generated from BuLi (1.6 M in hexanes, 1.6 mL) and diisopropylamine (0.35 mL). TTF−Li yellow precipitate formed slowly. After the solution was stirred for 1 h, chlorodiethylphosphine (0.34 mL, 2.5 mmol) (for PEt_2-TTF) or dichloroethylphosphine (0.14 mL, 1.3 mmol) (for $PEtTTF_2$) was added dropwise, and the reaction temperature was allowed to rise slowly overnight to room temperature. The reaction mixture was then filtered through Celite in toluene. Evaporation under reduced pressure yielded an orange oil in both cases. Elution on silica gel with a mixture of cyclohexane:dichloromethane (3:1 v:v) eliminated unreacted TTF and yielded PEt_2TTF as a yellow liquid (50% yield).[34]

Synthesis of $W_6S_8(PEt_2TTF)_6$. $W_6S_8(4\text{-tbp})_6$ (0.5 g, 0.23 mmol) was loaded into a 25 mL Schlenk tube equipped with a Teflon stir bar, and a solution of 0.722 g (2.47 mmol) PEt_2TTF diluted in 10 mL of benzene was added. The tube was then sealed and placed in an oil bath set at 100 °C for 72 h. A green precipitate formed upon stirring. The precipitate was then filtered inside the glovebox, washed with 10 mL of benzene and 6 mL of diethyl ether

(13) Mizutani, J.; Amari, S.; Imoto, H.; Saito, T. *J. Chem. Soc., Dalton Trans.* **1998**, 819−824.
(14) Magliocchi, C.; Xie, X.; Hughbanks, T. *Inorg. Chem.* **2000**, *39*, 5000−5001.
(15) Mironov, Y. V.; Virovets, A. V.; Naumov, N. G.; Ikorskii, V. N.; Fedorov, V. E. *Chem.−Eur. J.* **2000**, *6*, 1361−1365.
(16) Jin, S.; Popp, F.; Boettcher, S. W.; Yuan, M.; Oertel, C. M.; DiSalvo, F. J. *J. Chem. Soc., Dalton Trans.* **2002**, 3096−3100.
(17) Saito, T.; Yoshikawa, A.; Yamagata, T.; Imoto, H.; Unoura, K. *Inorg. Chem.* **1989**, *28*, 3588−3592.
(18) Ehrlich, G. M.; Warren, C. J.; Vennos, D. A.; Ho, D. M.; Haushalter, R. C.; DiSalvo, F. J. *Inorg. Chem.* **1995**, *34*, 4454−4459.
(19) Xie, X.; McCarley, R. E. *Inorg. Chem.* **1995**, *34*, 6124−6129.
(20) Xie, X.; McCarley, R. E. *Inorg. Chem.* **1997**, *36*, 4665−4675.
(21) Venkataraman, D.; Rayburn, L. L.; Hill, L. I.; Jin, S.; Malik, A.-S.; Turneau, K. J.; DiSalvo, F. J. *Inorg. Chem.* **1999**, *38*, 828−830.
(22) Jin, S.; Zhou, R.; Scheuer, E. M.; Adamchuk, J.; Rayburn, L. L.; DiSalvo, F. J. *Inorg. Chem.* **2001**, *40*, 2666−2674.
(23) Oertel, C. M.; Sweeder, R. D.; Patel, S.; Downie, C. M.; DiSalvo, F. J. *Inorg. Chem.* **2005**, *44*, 2287−2296.
(24) Saito, T.; Yamamoto, N.; Yamagata, T.; Imoto, H. *J. Am. Chem. Soc.* **1988**, *110*, 1646−1647.
(25) Chevrel, R.; Sergent, M.; Prigent, J. *J. Solid State Chem.* **1971**, *3*, 515−519.
(26) Peña, O.; Sergent, M. *Prog. Solid State Chem.* **1989**, *19*, 165−281.
(27) Jin, S.; DiSalvo, F. J. *Chem. Mater.* **2002**, *14*, 3448−3457.
(28) Malik, A.-S. Ph.D. Thesis, Cornell University, Ithaca, NY, 1998.
(29) Jin, S. Ph.D. Thesis, Cornell University, Ithaca, NY, 2002.
(30) Hill, L. I. Ph.D. Thesis, Cornell University, Ithaca, NY, 2000.
(31) Fourmigué, M.; Batail, P. *J. Chem. Soc., Chem. Commun.* **1991**, 1370−1372.
(32) Hill, L. I.; Jin, S.; Zhou, R.; Venkataraman, D.; DiSalvo, F. J. *Inorg. Chem.* **2001**, *40*, 2660−2665.
(33) Fourmigué, M.; Batail, P. *Bull. Soc. Chim. Fr.* **1992**, *129*, 29−36.
(34) In the case of $PEtTTF_2$, it is very hard to separate the product by just running the reaction mixture through a silica gel column. Instead, high performance liquid chromatography (HPLC) has to be employed to separate this product out, with a solvent mixture of cyclohexane and dichloromethane (4:1 v:v).

Table 1. Crystallographic Data for Three $W_6S_8(PEt_2TTF)_6$ Polymorphs (1−3) and $W_6S_8(PEtTTF_2)_6$ (4)

	1	2	3	4
chemical formula	$C_{60}H_{78}P_6S_{32}W_6$	$C_{84}H_{102}P_6S_{32}W_6$	$C_{84}H_{102}P_6S_{32}W_6$	$C_{124}H_{146}O_{10}P_6S_{56}W_6$
fw	3114.06	3426.50	3426.50	4880.85
space group	$P\bar{1}$	$P\bar{1}$	$R\bar{3}$	$P\bar{1}$
a (Å)	12.415(11)	14.0512(10)	23.659(3)	16.8243(13)
b (Å)	12.620(2)	15.1392(10)	23.659(2)	17.4251(13)
c (Å)	14.550(10)	15.1699(10)	16.9604(18)	18.9027(14)
α (deg)	86.51	61.6172(13)	90	106.185(2)
β (deg)	84.536(15) 90	84.3734(14)	90	101.500(2)
γ (deg)	87.16	84.1186(16)	120	112.613(2)
V (Å^3)	2263(5)	2819.7(3)	8221.9(15)	4609.8(6)
Z	1	1	3	1
T (K)	293(2)	173(2)	173(2)	173(2)
λ (Å)	0.91600	0.71073	0.71073	0.71073
ρ_{calcd} (g/cm^3)	2.285	2.018	1.815	1.729
μ (mm^{-1})	8.475	6.813	7.010	4.461
R_1[a] ($I > 2\sigma$/all)	0.0481/0.0482	0.0361/0.0527	0.0388/0.0588	0.0777/0.1585
wR_2[b] ($I > 2\sigma$/all)	0.1350/0.1352	0.0772/0.0931	0.0880/0.0969	0.1922/0.2399

[a] $R_1 = \sum||F_o| - |F_c||/\sum|F_o|$. [b] $wR_2 = [\sum w(F_o^2 - F_c^2)^2/\sum w(F_o^2)^2]^{1/2}$.

Table 2. Selected Bond Lengths (Å) and Angles (deg) for Clusters 1−4

	1	2	3	4
W−W range	2.672(3)−2.685(2)	2.6717(3)−2.6913(3)	2.6775(5)−2.6817(5)	2.6685(14)−2.6824(14)
W−S range	2.446(3)−2.473(3)	2.4361(15)−2.4624(13)	2.441(2)−2.4572(17)	2.439(5)−2.479(6)
W−P range	2.518(4)−2.537(3)	2.5411(15)−2.5671(17)	2.551(2)	2.524(6)−2.534(6)
W−W−W range[a]	89.63(4)−90.37(4)	89.689(10)−90.310(10)	90.0	89.95(4)−90.05(4)
W−W−W range[b]	59.84(5)−60.21(5)	59.622(8)−60.345(8)	59.948(8)−60.108(16)	59.74(4)−60.21(3)

[a] Within equatorial squares. The mean W−W−W angle is constrained to 90° if the cluster is centered on an inversion center. [b] Within triangular faces. The mean W−W−W angle is automatically 60° by geometry.

consecutively, and allowed to dry. The yield of $W_6S_8(PEt_2TTF)_6$ was 0.67 g (85%). $^{31}P\{^1H\}$ NMR (C_6D_6): δ −11.6. ^1H NMR: δ 7.4 (1H, d, $J_{H-P} = 9$ Hz), 5.4 (2H, m), 2.1 (4H, broad, $-CH_2-$), 1.2 (6H, m, Me). This cluster was found to crystallize into three polymorphs in different trials of recrystallization, namely, $P\bar{1}$ $W_6S_8(PEt_2TTF)_6$ (**1**), $P\bar{1}$ $W_6S_8(PEt_2TTF)_6\cdot 4C_6H_6$ (**2**), and $R\bar{3}$ $W_6S_8(PEt_2TTF)_6\cdot 4C_6H_6$ (**3**). Single crystals of **1** were obtained by recrystallization of the $W_6S_8(PEt_2TTF)_6$ powder in toluene. The solution was heated at 100°C for a few hours and then allowed to gradually cool to room temperature over a day to give suitable size crystals for X-ray diffraction study. Single crystals of both **2** and **3** were obtained by recrystallization of the $W_6S_8(PEt_2TTF)_6$ powder in benzene in a fashion similar to that of **1**. Anal. Calcd for **1**: C, 23.14; H, 2.53; S, 32.95. Found: C, 25.64; H, 2.21; S, 31.06. Anal. Calcd for **2**: C, 29.44; H, 3.01; S, 29.95. Found: C, 28.18; H, 2.60; S, 30.27. Anal. Calcd for **3**: C, 29.44; H, 3.01; S, 29.95. Found: C, 27.96; H, 2.45; S, 30.15.

Synthesis of $W_6S_8(PEtTTF_2)_6$ (4). $W_6S_8(4\text{-tbp})_6$ (0.084 g, 0.0387 mmol) was loaded into a 25 mL Schlenk tube equipped with a Teflon bar, and a solution of 0.22 g (0.471 mmol) of $PEtTTF_2$ diluted in 8 mL of benzene was added. The tube was then sealed and placed in an oil bath set at 100 °C for 72 h upon stirring. A greenish yellow precipitate was filtered inside the glovebox, washed with 10 mL of benzene and 8 mL of ethyl ether consecutively, and allowed to sit and dry. Crystalline powder was collected and weighed at 0.131 g (81.4% yield). $^{31}P\{^1H\}$ NMR (THF-d_8): δ −18.9. ^1H NMR: δ 7.15 (2H, d, $J_{H-P} = 9$ Hz), 6.5 (4H, m), 2.5 (2H, broad, $-CH_2-$), 1.3 (3H, broad, Me). A single crystal of $W_6S_8(PEtTTF_2)_6\cdot 10THF$ was grown by recrystallization of the product powder in THF. The THF solution was heated at 95 °C for a few hours and slowly cooled over a day. This process was repeated several times to give a single crystal with a suitable size for X-ray diffraction measurements. Anal. Calcd for $W_6S_8(PEtTTF_2)_6$: C, 24.25; H, 1.60; S, 43.16. Found: C, 25.52; H, 1.79; S, 40.85.

Chemical Oxidation of $W_6S_8(PEt_2TTF)_6$. $W_6S_8(PEt_2TTF)_6$ (0.1 g, 0.032 mmol) was loaded into a Schlenk tube equipped with a Teflon stir bar and dissolved in 20 mL of benzene. To the solution was added a solution of 0.07 g (0.21 mmol) of $[Cp_2Fe]PF_6$ dissolved in 12 mL of CH_2Cl_2. The tube was then sealed, and the mixture was allowed to react upon stirring at room temperature. A brown precipitate formed during the second day of the reaction, and the reaction was allowed to continue for 4 days. The precipitate was then filtered inside the glovebox and washed with 15 mL benzene, followed by copious amounts of CH_2Cl_2 until the filtrate was colorless. After being washed with 8 mL of diethyl ether, the powder was allowed to sit and dry and weighed 0.11 g (yield 89.2%).

X-ray Structure Determination. Single-crystal X-ray diffraction data on clusters **2**−**4** were collected on a Bruker SMART system with a CCD detector using Mo Kα radiation. Crystals were mounted on a thin glass fiber using polybutene oil and were immediately cooled in a cold N_2 stream, and the data were collected at 173 K. The cell constants were determined from more than 50 well-centered reflections. The data were integrated using SAINT software.[35] The structures were solved using SHELXS and refined using the full-matrix least-squares method on F_o^2 with SHELXL software packages.[36] Empirical absorption corrections were applied using the SADABS program.[37] All refinements converged, and the residual electron densities were near the W atoms. In **2** and **3**, all non-hydrogen atoms were refined anisotropically except atoms from solvent molecules, which were refined isotropically. In **4**, all nonsolvent non-hydrogen atoms were refined anisotropically except four carbon atoms from the TTF moieties, which were refined isotropically. Solvent molecules in **4** were also refined with isotropic thermal parameters. The crystallographic data are listed in Table 1. Selected bond lengths and angles for clusters **2**−**4** are listed in Table 2.

(35) *SAINT Plus: Software for the CCD Detector System*; Bruker Analytical X-ray System: Madison, WI, 1999.
(36) Sheldrick, G. M. *SHELXL*, version 5.10; Siemens Analytical X-ray Instruments, Inc.: Madison, WI, 1999.
(37) Sheldrick, G. M. *SADABS* (the computer program SADABS is used by Siemens CCD diffractometers); Institute für Anorganische Chemie der Universität Göttingen: Göttingen, Germany, 1999.

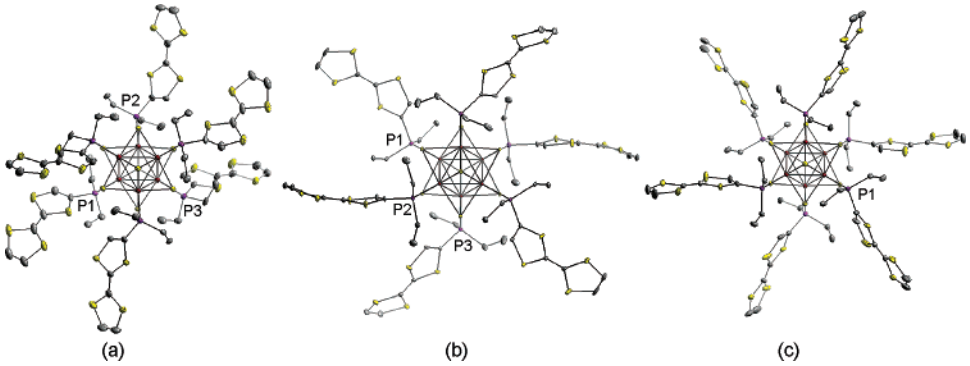

Figure 1. Molecular Structures of clusters **1**−**3** showing the different arrangements of TTF moieties around the W_6S_8 core in the three polymorphs of the $W_6S_8(PEt_2TTF)_6$ cluster (view down the octahedron $\bar{3}$ axis for all three). H atoms are omitted for clarity. Ligand PEt_2TTF is linked to W_6S_8 via the P−W bond. W, red; S, yellow; P, magenta; C, gray. The thermal ellipsoids are drawn at the 90% probability level. (a) Cluster **1** ($P\bar{1}$ structure without solvent); (b) cluster **2** ($P\bar{1}$ with solvent benzene); (c) cluster **3** ($R\bar{3}$ with solvent benzene).

Structure Determination from CHESS. Single-crystal diffraction data on cluster **1** were obtained from CHESS (Cornell High Energy Synchrotron Source). Diffraction was carried out using the CHESS F-1 beam line with Area Detector Systems CCD.[38] Data were processed with the HKL processing package (xdisp/denzo/scalepack).[39] The structure was solved using SHELXS and refined using the full-matrix least-squares method on F_o^2 with SHELXL software packages.[36] In **1**, all non-hydrogen atoms were refined with anisotropic thermal parameters. The crystallographic data are listed in Table 1. Selected bond lengths and angles for cluster **1** are listed in Table 2.

Electrochemistry Study of Clusters. Cyclic voltammetry of the ligand PEt_2TTF and the cluster $W_6S_8(PEt_2TTF)_6$ was performed using an Ensman EI-400 Potentiostat driven by an EG&G PARC 175 Universal Programmer, in a three compartment electrochemical cell. A 0.1 M $(Bu_4N)PF_6$ solution in anhydrous benzonitrile was used as supporting electrolyte for all experiments. The solution concentrations were around 10 mM for the free ligand and 1 mM for the cluster complex. A Pt disk electrode (3 mm diameter) was used as the working electrode and a Pt coil as the counter electrode. All potentials are referenced to Ag/AgCl (saturated NaCl) unless otherwise stated. The solutions were degassed with high-purity N_2 for 10 min before measurements.

IR and XPS Characterizations. Infrared (IR) and X-ray photoelectron spectroscopy (XPS) measurements were performed on both the $W_6S_8(PEt_2TTF)_6$ cluster and its oxidized product. Transmission FT-IR spectra were acquired with a Bruker IFS 66/S spectrometer over two ranges (4000−400 and 680−200 cm^{-1}). Mid-IR samples were prepared as CsI pellets (the pellets were pressed from a mixture of a 1.5 mg sample and 225 mg of CsI). Far-IR samples were prepared as Nujol mulls between CsI windows. The mid-IR spectra were run for 100 scans at a resolution of 4 cm^{-1}, and the far-IR spectra were run for 400 scans at a resolution of 6 cm^{-1}. XP spectra were collected with a Kratos Analytical AXIS Ultra system equipped with a monochromatic aluminum (1486.6 eV) X-ray source. The powder samples were pressed into 3M double-sided tape using a mortar and pestle and fastened to the sample platen using conductive carbon tape. Binding energies (BEs) were calibrated with C 1s BE = 285 eV.

Electrical Conductivity Measurements. Electrical conductivity measurements were performed on pressed pellets of both the neutral cluster complex $W_6S_8(PEt_2TTF)_6$ and the oxidized powder $W_6S_8(PEt_2TTF)_6{\cdot}xPF_6$ ($x \approx 5$). The 1/4 in. diameter cylindrical pellet was contacted by a linear array of four spring-loaded gold pins. The measured resistance was converted to conductivity by comparison with the resistance of a pure copper sample of the same dimensions.

Results and Discussion

Polymorphs of $W_6S_8(PEt_2TTF)_6$ (1−3). Ligand-exchange reactions of the precursor cluster W_6S_8(4-*tert*-butylpyridine)$_6$ with excess PEt_2TTF ligands in benzene at 100 °C yielded the $W_6S_8(PEt_2TTF)_6$ cluster. Three polymorphs of $W_6S_8(PEt_2TTF)_6$ were identified as the results of different trials of recrystallization efforts, namely, $P\bar{1}$ without solvent (**1**), $P\bar{1}$ with four benzene solvent molecules per W_6S_8 cluster (**2**), and $R\bar{3}$ with the same number of solvent benzene molecules (**3**). These three polymorphs were obtained in different attempts to grow single crystals from different solvents: toluene (**1**) or benzene (**2** and **3**). Powder X-ray diffraction patterns of each polymorph were taken from their bulk samples and compared to the theoretical powder patterns simulated from their single-crystal structures. Good agreement between the experimental and theoretical powder patterns indicated the bulk samples were obtained as crystalline and single-phase materials. (Powder patterns are available in the Supporting Information).

A single crystal of **1** ($W_6S_8(PEt_2TTF)_6$) was grown by slow cooling of $W_6S_8(PEt_2TTF)_6$ in toluene. **1** crystallizes in the triclinic space group $P\bar{1}$, with one cluster molecule sitting on an inversion center in the unit cell. The cluster has an octahedral core of six tungsten atoms; it is face-capped by eight sulfur atoms and has six terminal TTF derivative ligands coordinated to tungsten atoms through the phosphorus atoms. The molecular structure of cluster **1** is shown in Figure 1a.

The average W−P distance in **1** is 2.526 Å, slightly shorter than that observed in **2** (2.550Å) and **3** (2.551 Å). As usually encountered in neutral TTF species, the three independent TTF ligand moieties in cluster **1** are not flat. Instead, the two halves of the fulvalene rings are distorted to give rise to an overall boat conformation. TTFs attached to P1 (W−P = 2.518 Å) have the most-bent geometry of the three TTF environments. C3 and C4 atoms deviate from the central plane (defined by S1, S2, and C1 atoms, see Figure 2 for the TTF atomic numbering scheme) by 0.57 and 0.53 Å,

(38) Szebenyi, D. M. E.; Arvai, A.; Ealick, S.; LaIuppa, J. M.; Nielsen, C. *J. Synchrotron Radiat.* **1997**, *4*, 128−135.
(39) Otwinowski, Z.; Minor, W. *Processing of X-ray Diffraction Data Collected in Oscillation Mode*; Academic Press: New York, 1997; Vol. 276.

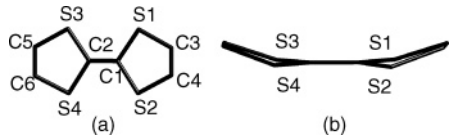

Figure 2. (a) Atomic numbering of the TTF moiety. C5 is attached to the P atom in the ligand. (b) Boatlike conformation of TTF moieties.

respectively, whereas C5 and C6 atoms deviate from the plane (defined by S3, S4, and C2 atoms) by 0.54 and 0.51 Å, respectively. TTFs attached to P3, with the longest W−P distance (2.537 Å), also have the flattest geometry of the three, with deviations from planes at 0.048, 0.045, 0.044, and 0.065 Å for C3, C4, C5, and C6, respectively. TTFs attached to P2 (W−P = 2.523 Å) have an unsymmetrical bent geometry, with C5 and C6 deviating at 0.50 and 0.49 Å, respectively, whereas C3 and C4 deviate at only 0.28 and 0.29 Å, respectively. Because the energy difference between planar and boatlike TTF conformations is very small,[40] TTF geometries in different compounds are relatively flexible and can appear in various conformations depending on the electronic interaction and steric arrangements, as observed in this structure.

Polymorph **2** ($W_6S_8(PEt_2TTF)_6 \cdot 4C_6H_6$) also has a triclinic $P\bar{1}$ structure. There is one $W_6S_8(PEt_2TTF)_6$ cluster with four benzene solvent molecules in one unit cell. The cluster sits on the inversion center, and the solvent benzene molecules sit on general positions. W−P distances in this cluster range from 2.541 to 2.567 Å. The three crystallographically independent pairs of TTF moieties on the cluster ligands have slightly different bent geometries. For TTFs attached to P2 (W−P = 2.567 Å), atoms C3−C6 have an average deviation of 0.434 Å from the central planes (same definition as in cluster **1**, see Figure 2 for the TTF atomic numbering). For TTFs linked to P3 (W−P = 2.542 Å), this value is 0.489 Å. For TTFs with the shortest W−P linkage of the three (W−P = 2.541 Å), the two halves of the TTF are bent unsymmetrically. C3 and C4 have an average of 0.363 Å deviation, whereas C5 and C6 have a much longer deviation of 0.602 Å from the central plane. See Figure 1b for the molecular structure of cluster **2**.

Polymorph **3** ($W_6S_8(PEt_2TTF)_6 \cdot 4C_6H_6$) also crystallized out with four benzene solvent molecules, but in an $R\bar{3}$ symmetry setting. There are three cluster units and 12 benzene molecules per hexagonal unit cell. $W_6S_8(PEt_2TTF)_6$ sits on the 3-fold inversion axes. All six phosphine−TTF ligands are in the same coordination environment because of the $\bar{3}$ symmetry. The W−P distance in this cluster is 2.551 Å. TTFs in this cluster are still in a slightly unsymmetrical bent geometry: the deviation of C3, C4, C5, and C6 is 0.207, 0.277, 0.159, and 0.175 Å, respectively. The molecular structure of the $R\bar{3}$ $W_6S_8(PEt_2TTF)_6$ cluster is shown in Figure 1c.

$W_6S_8(PEtTTF_2)_6 \cdot 10THF$ (4). Bis-TTF-ligated cluster $W_6S_8(PEtTTF_2)_6$ was obtained as a powder product in a similar ligand-exchange reaction from W_6S_8(4-*tert*-butylpyridine)$_6$ with excess $PEtTTF_2$ ligand at 100 °C in benzene. The product powder was recrystallized in THF to give the single crystal $W_6S_8(PEtTTF_2)_6 \cdot 10THF$. The cluster complex crystallized in a $P\bar{1}$ setting, with one $W_6S_8(PEtTTF_2)_6$ cluster on the inversion center and 10 THF solvent molecules on general positions per triclinic unit cell. The average W−P distance in this cluster is 2.529 Å. As observed in mono-TTF-ligated clusters **1**−**3**, TTF molecules in this cluster also exhibit nonplanar boatlike conformations, vide supra. To the best of our knowledge, this is the first reported structure of a metal-cluster complex with 12 TTF moieties attached to one cluster unit. The molecular structure of cluster **4** is shown in Figure 3.

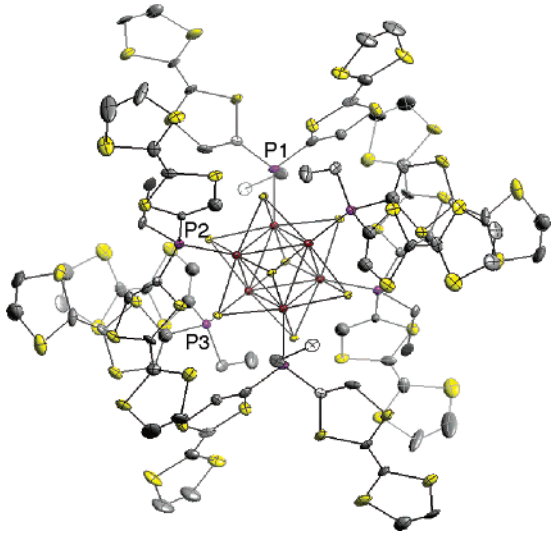

Figure 3. Molecular structure of cluster $W_6S_8(PEtTTF_2)_6$. H atoms are omitted for clarity. W, red; S, yellow; P, magenta; C, gray. The thermal ellipsoids are drawn at the 90% probability level.

One- and Two-Dimensional Intercluster TTF Interactions. As our eventual goal is to build high-dimensional conductive networks of TTF clusters, we are structurally interested in the intercluster TTF close π-contacts. These TTF π-couplings serve as bridges between neighboring cluster units, and high dimensionality can be achieved with the aid of such interactions.

Good TTF π-contacts are found in cluster **1** ($W_6S_8(PEt_2TTF)_6$) and cluster **4** ($W_6S_8(PEtTTF_2)_6 \cdot 10THF$). In **1**, there is one cluster in each triclinic unit cell. TTF moieties attached to P2 (W−P = 2.523 Å) from neighboring clusters form cofacial pairs (see Figure 4a). These TTF dimers extend in the *bc* plane. The stacking within these dimers was examined and found to be of a double-bond over ring type overlap.[41] The closest C···C distance between two TTF molecules is 3.37Å (see Figure 5a). This double-bond over ring type of overlap is common in TTF chemistry, as in the well-known TTF−TCNQ charge-transfer complexes (where the closest C···C distance is 3.47 Å),[42,41] in neutral TTF molecules (3.62 Å),[43] and also between TTF^0−TTF^+ molecules in mixed-valence species (3.48 Å).[44] The C···C closest distance

(40) Katan, C. *J. Phys. Chem. A* **1999**, *103*, 1407−1413.

(41) Kistenmacher, T. J.; Phillips, T. E.; Cowan, D. O. *Acta Crystallogr., Sect. B* **1974**, *30*, 763−768.
(42) Phillips, T. E.; Kistenmacher, T. K.; Ferraris, J. P.; Cowan, D. O. *Chem. Commun.* **1973**, 471−472.
(43) Cooper, W. F.; Kenny, N. C.; Edmonds, J. W.; Nagel, A.; Wudl, F.; Coppens, P. *Chem. Commun.* **1971**, 889−890.
(44) Legros, J.-P.; Bousseau, M.; Valade, L.; Cassoux, P. *Mol. Cryst. Liq. Cryst.* **1983**, *100*, 181−192.

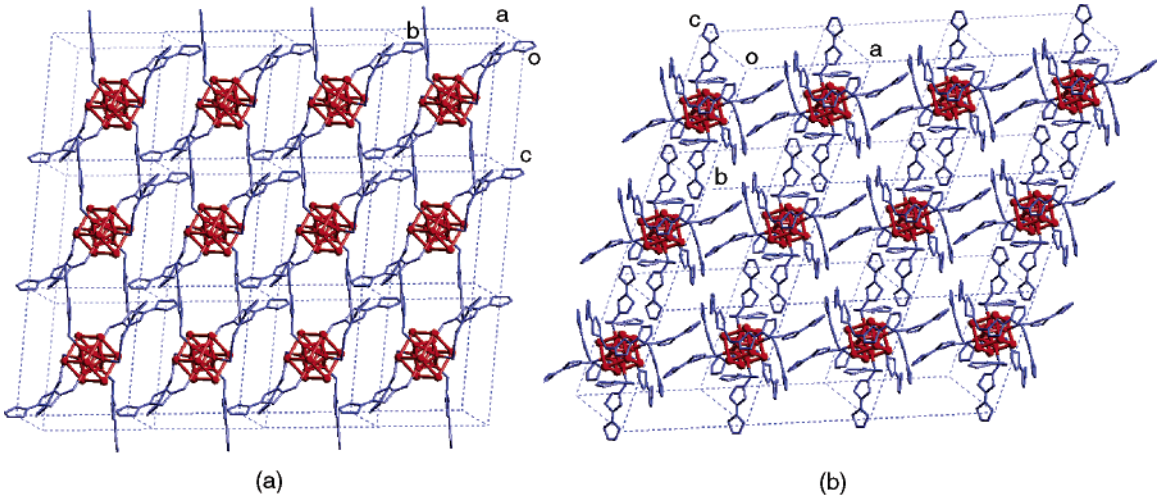

Figure 4. Crystal packing and TTF close contacts in clusters **1** and **4**. W_6S_8 octahedral cores are pictured in red, and the TTF−phosphine ligands are pictured in blue. (a) Cluster **1**, $W_6S_8(PEt_2TTF)_6$; (b) cluster **4**, $W_6S_8(PEtTTF_2)_6$·10THF. Solvent THF molecules are omitted for clarity.

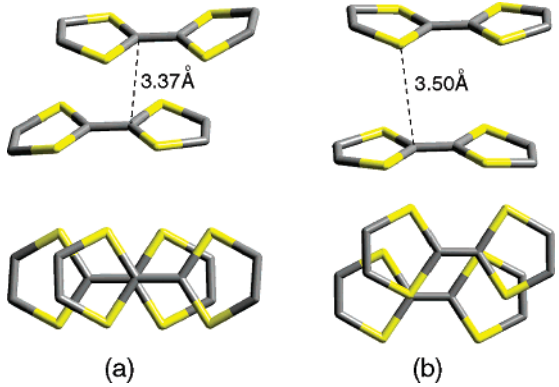

Figure 5. Two modes of TTF intradimer stacking geometries observed in clusters **1** and **4**. (a) Stacking of double-bond over ring, as observed in cluster **1**; (b) stacking of slip−overlap, as observed in cluster **4**.

observed in this structure is considerably shorter than in other systems with the same TTF stacking mode, as mentioned above. In fact, this distance is comparable to the distance observed between TTF^+−TTF^+ molecules in mixed-valence species (3.40 Å),[44] indicating a stronger interaction between TTF moieties. These close TTF $\pi-\pi$ contacts bridge neighboring clusters with good intercluster communication in one dimension, and it's obvious that such interactions would be important for charge-carrier traveling in a partially oxidized cluster. The packing diagram of cluster **1** showing intercluster TTF stacking in one dimension is depicted in Figure 4a.

We can obtain a rough measure of the strength of the intracluster interactions (through the W_6S_8 core) vs intercluster TTF π-interactions through an eH calculation using standard atomic parameters.[45] Intracluster interactions gave the HOMO of the TTF moiety a spread of a little more than 0.2 eV, whereas the intercluster π-interactions gave a significantly smaller dispersion.

By increasing the TTF content in the cluster, we hope to promote more TTF interactions and coupling in all dimensions. In the crystal structure of cluster $W_6S_8(PEtTTF_2)_6$, with 12 TTF molecules attached to one W_6S_8 core, the probability of more and larger intercluster interactions through TTF molecules is significantly improved. As Figure 4b shows, intercluster TTF interactions exist in two dimensions in cluster **4**, even though there are a large number of THF solvent molecules of crystallization in the product. TTF molecules from nearby clusters stack in pairs in the *ab* and *bc* planes. See Figure 4b for the packing diagram of cluster **4** showing intercluster TTF contacts in two dimensions. We expect that the number of intercluster TTF contacts could be increased in $W_6S_8(PEtTTF_2)_6$ if the THF molecules of crystallization were removed. However, we have not yet obtained a single crystal of the $W_6S_8(PEtTTF_2)_6$ cluster without solvents of crystallization, because of the poor solubility of this cluster in other common organic solvents.

The stacking mode of TTF dimers in the $W_6S_8(PEtTTF_2)_6$·10THF cluster is called the slip−overlap type, where the two TTF molecules in the dimer are shifted away from each other along the short molecular axis and there is a partial intradimer ring overlap. The shortest intradimer contact is the C···S distance, at about 3.50 Å for both pairs of TTF dimers extending in two dimensions. Again, these TTF close contacts are important in bridging neighboring clusters and would be expected to act as passage for clusters to communicate with one another in an oxidized network structure. The two modes of TTF intradimer stacking geometries observed in clusters **1** and **4** are shown in Figure 5.

Clusters Assemble in Closest-Packing Patterns. In the introduction, we noted that the fcc closest-packing structures of superconducting fullerides exemplify the geometrical ease of molecules of high symmetry to assemble in closest packings, where each molecule maintains good intermolecular contacts with multiple closest neighbors. As we mentioned, one of our major motivations in exploiting the M_6S_8 clusters as the building units is the increased likelihood of these highly symmetrical clusters to adopt closest-packing structures. Our results presented here support this crystal design idea.

Rhombohedral cluster **3** crystallized into a distinct ABC closest-packing structure, as shown in Figure 6. The clusters arrange themselves in ABC closest-packing layers (squashed along the packing direction, thus not the fcc structure). Because of this squashed ABC packing, each cluster is

(45) Landrum, G. *YAeHMOP*, version 3.0.1; http://yaehmop.sourceforge.net.

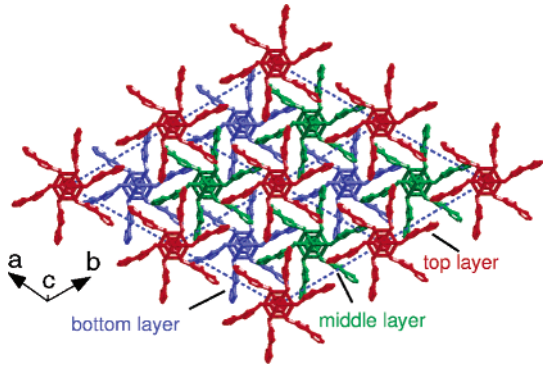

Figure 6. Observed crystal structure of **3** ($R\bar{3}$, $W_6S_8(PEt_2TTF)_6 \cdot 4C_6H_6$). Solvent benzene molecules are omitted for clarity. Clusters adopt an ABC closest packing.

further from its six neighbors in the same layer (closest intermolecular distance at 6.47 Å) than from its six closest neighbors, three each from the layer above and below (closest intermolecular distance 3.55 Å). Moreover, each cluster from layer A (or B, C) is also in close contact with two overlapping clusters (closest intermolecular distance 8.23 Å), one each from the upper and lower next layer A (or B, C). Each cluster therefore has fourteen close neighbors, six from the same layer and eight from different layers. (The void space formed between each cluster and its eight neighbors at different layers was taken by a solvent benzene molecule, thus giving the 1:4 cluster:solvent ratio.)

Examinations of the crystal structures of clusters $W_6S_8(PEt_2TTF)_6$ (**1**) and $W_6S_8(PEtTTF_2)_6$ (**4**) revealed similar ABC patterns, where each cluster has six closest neighbors from the upper and lower layers and an additional group of six neighbors from the same layer with slightly longer distances. Figure 7 illustrates the ABC setting observed in both clusters **1** and **4**. In an ideal ABC closest packing, each molecule has 12 nearest neighbors at equal distances, whereas in the cluster structures discussed here, different degrees of deviation from the ideal case are observed, because of the contractions along the stacking direction. Thus the 12 neighbors are not isotropically distributed around each cluster. (The neighbors from the same layer are situated further apart.) Nevertheless, the advantage of organizing the cluster molecules into an ABC closest-packing fashion is that this pattern would optimize the number of close neighbors each cluster can have, thus improving the amount of intermolecular contacts substantially.

One important structural difference of cluster **3** and clusters **1** and **4** is that in cluster **3**, the cofacial stacks of TTF molecules, so ubiquitous in TTF chemistry, have been entirely suppressed. The solvent benzene molecules, in conjunction with the C−H···S bonds, which may be energetically comparable with the cofacial TTF $\pi-\pi$ contacts, have dominated the overall crystal structure in cluster **3** (Figure 6), and this cluster does not exhibit the close TTF pairs seen in both clusters **1** and **4**. Thus, although the clusters form closest ABC packing in **3**, which is reminiscent of the fulleride structures, they need further intercluster contacts through TTF molecules to build extended interactions between each other. Not surprisingly, this same suppression of the cofacial TTF contacts is also observed in the structure of cluster **2**, a polymorph with exactly the same composition and number of solvent molecules as those of cluster **3**.

Cyclic Voltammetry Studies. Cyclic voltammetry (CV) studies were performed on cluster $W_6S_8(PEt_2TTF)_6$ and free ligand PEt_2TTF in benzonitrile at room temperature (Figure 8). The cyclic voltammogram of cluster $W_6S_8(PEt_2TTF)_6$ exhibits two oxidation waves, corresponding to the generation of the radical cation (TTF^+) at $E_{1/2} = 0.45$ V and the dication (TTF^{2+}) at $E_{1/2} = 0.87$ V, respectively. (Compared to the CV of free ligand PEt_2TTF at $E_{1/2} = 0.50$ V and $E_{1/2} = 0.93$ V.) In both the TTF-bound cluster and the free-ligand cyclic voltammograms, we observed an irreversible reduction at −0.45 V for the cluster complex and at −0.3 V for the free ligand. To the best of our knowledge, a similar feature has not been noted in previous electrochemical studies on TTF−phosphine compounds.[33,46] One tentative explanation for this observation has to do with the phosphorus participation in the oxidation process. Even in the cluster complex where the ligand PEt_2TTF is bonded to W through P and therefore no lone pair of electrons resides on P, it seems that phosphorus is not innocent of oxidation, presumably because of the presence of TTF, which facilitates the charge transfer between the phosphorus atom and the nearby TTF moiety.[47]

The W_6S_8 metal cluster is known to exhibit both reversible one-electron oxidation and reversible one-electron reduction near 0.12 and −1.0 V, respectively.[17,21] It is also known that a second irreversible oxidation of this cluster occurs around 0.8 V, which has not yet been well-characterized.[21] In the case of our cluster, we did observe the reversible redox couple near −0.9 V, which corresponds to the one-electron reduction of W_6S_8. (Because of the 1:6 ratio of W_6S_8 core and TTF ligands, this couple is not prominent on the full cyclic voltammogram, whereas a small-region scan at negative potentials reveals the fine feature of this reversible pair of peaks. See Figure 8, left inset.) However, we were not able to identify a separate W_6S_8 first oxidation couple from the cyclic voltammogram. This may suggest some kind of coupling between the W_6S_8 cluster core and the TTF ligands, and the redox couple near 0.47 V is likely to be a mingled feature from the contributions of both the cluster core and the TTF ligands.[48] The presence of possible phosphorus participation in oxidation further complicated the process and did not allow for an accurate measure of the number of electrons involved in this oxidation step.

(46) Gerson, F.; Lamprecht, A.; Fourmigué, M. *J. Chem. Soc., Perkin Trans. 2* **1996**, 1409−1414.

(47) More CV experiments were carried out to investigate this extra reduction peak near −0.3 V. See the Supporting Information for details of the electrochemical studies.

(48) Extended Hückel calculations using default W, S, P, C, and H parameters give an alternate explanation of the CV curves (see ref 45 for eH parameters). The eH calculations suggest that in its native form, $W_6S_8(PEt_2TTF)_6$ has both six high-lying occupied orbitals from −9.5 to −9.1 eV and two low-lying unoccupied orbitals from −9.1 to −9.0 eV. These eight orbitals correspond to the six HOMO orbitals of TTF (there are six TTF moieties per cluster) and the e_g LUMO orbitals of the $W_6S_8L_6$ cluster. eH calculations with standard parameters suggest that the two lowest-lying orbitals, i.e. −9.5 to −9.4 eV, are primarily of $W_6S_8L_6$ e_g provenance. Thus the TTF ligands in native $W_6S_8(PEt_2TTF)_6$ are partially oxidized. If these results are correct, we might not expect to see oxidation of the W_6S_8 cluster core, but we would observe facile reduction of $W_6S_8(PEt_2TTF)_6$ because of the low-lying mainly TTF orbitals. Unfortunately, the large size of the cluster does not allow for ab initio verification of this eH picture.

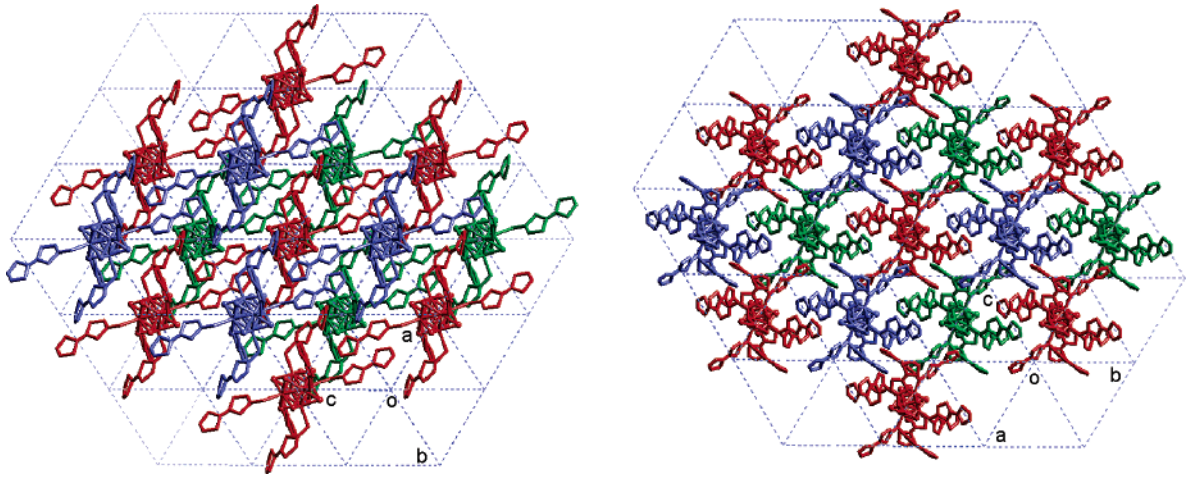

Figure 7. ABC patterns observed in the cluster structures **1** (left) and **4** (right). Blue, top layer; red, middle layer; green, bottom layer. Ethyl groups, all hydrogen atoms, and solvent THF molecules in cluster **4** are omitted for clarity.

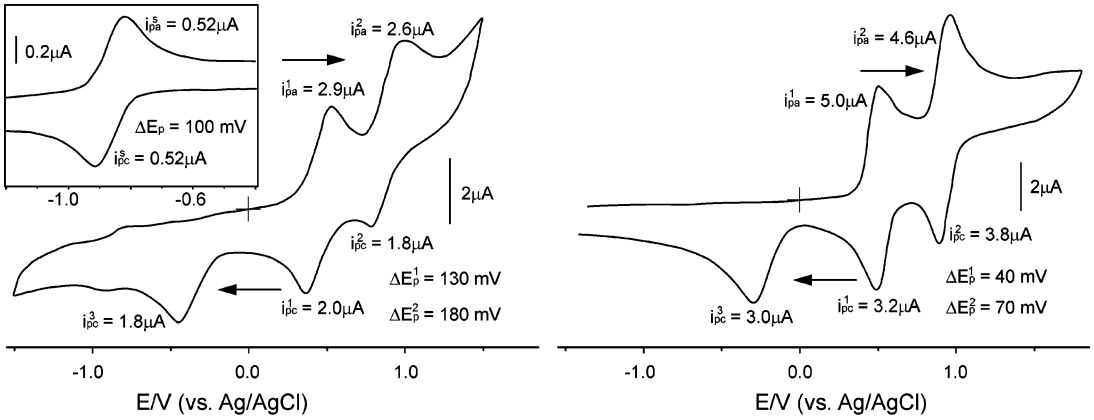

Figure 8. Cyclic voltammograms (scan rate of 100 mV/s) of cluster $W_6S_8(PEt_2TTF)_6$ (left) and free ligand PEt_2TTF (right) in benzonitrile. Both contain 0.1 M Bu_4NPF_6 electrolyte. For $W_6S_8(PEt_2TTF)_6$ (left), the inset pictures a small-range scan showing the reversible redox couple ($[W_6S_8]]/[W_6S_8]^-$) at −0.87 V. Both scans start at 0 V (shown in the picture as the cross sign), and the scan directions are also depicted.

In the cluster CV, the second TTF oxidation peak is less reversible compared to the same peak in free ligand PEt_2-TTF, as this overlaps with the onset of the irreversible oxidation of W_6S_8. Therefore, in our later efforts of oxidizing the cluster complex, we need an oxidizing agent with a reduction potential somewhere between 0.4 and 0.8 V, so that it is capable of oxidizing both W_6S_8 and TTF by one electron, but not so strong as to induce the irreversible oxidation of W_6S_8.

Oxidized $W_6S_8(PEt_2TTF)_6$. We have shown that inter-cluster interactions can be achieved by TTF−TTF close π-contacts. Neutral clusters, however, should have filled bands, leading to semiconducting or insulating behavior. Compounds in which the W_6S_8 inorganic core and the TTF derivative ligands are simultaneously oxidized and in which the π-systems of the TTF molecules are strongly electronically coupled should exhibit metallic conductivity. Through the intermediary of the inorganic core, the π-systems of the TTF molecules may also be indirectly coupled to one another. Because of the poor solubility of the $W_6S_8(PEtTTF_2)_6$ cluster in regular organic solvents, oxidation efforts were mainly focusing on the mono-TTF cluster $W_6S_8(PEt_2TTF)_6$, and an oxidized powder product was obtained from the chemical oxidation method.

The engagement of TTF and its derivatives in the construction of conducting molecular assemblies is not a new concept. In fact, a number of charge-transfer salts that contain TTF (derivative) molecules as radical cations and metal clusters as counteranions have been reported, with their room-temperature conductivity ranges from semiconducting to metallic.[49−55] As TTF donor moieties are not covalently linked to the metal-cluster counteranions in these complexes, any interactions between the two components have to be through space and therefore should be weak. A few compounds that directly attach the TTF (derivative) ligands to metal complexes have been reported.[56−58] Yet structures

(49) Fuchs, H.; Fuchs, S.; Polborn, K.; Lehnert, T.; Heidmann, C.-P.; Müller, H. *Synth. Met.* **1988**, *27*, A271−A276.
(50) Gomez-Garcia, C. J.; Coronado, E.; Triki, S.; Ouahab, L.; Delhaes, P. *Synth. Met.* **1993**, *55*−*57*, 1787−1790.
(51) Gomez-Garcia, C. J.; Borras-Almenar, J. J.; Coronado, E.; Delhaes, P.; Garrigou-Lagrange, C.; Baker, L. C. W. *Synth. Met.* **1993**, *55*−*57*, 2023−2027.
(52) Pénicaud, A.; Boubekeur, K.; Batail, P.; Canadell, E.; Auban-Senzier, P.; Jérome, D. *J. Am. Chem. Soc.* **1993**, *115*, 4101−4112.
(53) Batail, P.; Boubekeur, K.; Fourmigué, M.; Gabriel, J.-C. P. *Chem. Mater.* **1998**, *10*, 3005−3015.
(54) Perruchas, S.; Boubekeur, K.; Auban-Senzier, P. *J. Mater. Chem.* **2004**, *14*, 3509−3515.
(55) Llusar, R.; Triguero, S.; Uriel, S.; Coronado, C. V. E.; Gomez-Garcia, C. J. *Inorg. Chem.* **2005**, *44*, 1563−1570.
(56) Dai, J.; Munakata, M.; Ohno, Y.; Bian, G.-Q.; Suenaga, Y. *Inorg. Chim. Acta* **1999**, *285*, 332−335.
(57) Iwahori, F.; Golhen, S.; Ouahab, L.; Carlier, R.; Sutter, J.-P. *Inorg. Chem.* **2001**, *40*, 6541−6542.
(58) Perruchas, S.; Avarvari, N.; Rondeau, D.; Levillain, E.; Batail, P. *Inorg. Chem.* **2005**, *44*, 3459−3465.

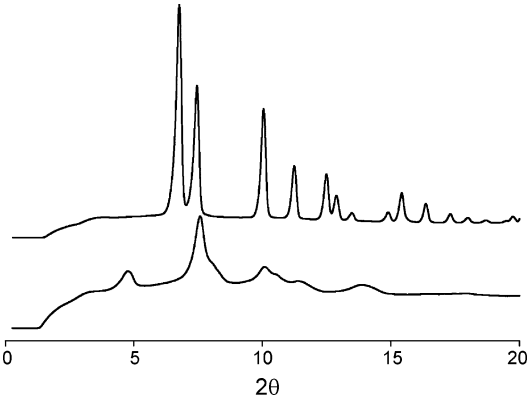

Figure 9. Powder patterns of oxidized cluster $[W_6S_8(PEt_2TTF)_6]]\cdot 5PF_6$ (bottom) and neutral cluster **3** $W_6S_8(PEt_2TTF)_6\cdot 4C_6H_6$ (top). Broad peaks from the oxidized cluster indicated poor crystallinity, and its similar low-angle diffractions suggested comparable cell dimensions with cluster **3**.

of radical cationic salts of this type remain scarce,[59] presumably because crystallization of such complex TTF systems is challenging. Indeed, despite numerous attempts with electrocrystallization techniques and chemical oxidation methods, we were not able to grow single crystals of the oxidized W_6S_8 TTF cluster. Instead, a poor crystalline powder product was obtained through the chemical oxidation of the $W_6S_8(PEt_2TTF)_6$ cluster.

Physical Characterization of the Oxidized Cluster. The chemical oxidation of $W_6S_8(PEt_2TTF)_6$ with ferrocenium hexafluorophosphate (reduction potential = 0.46 V vs Ag/AgCl) in a mixture solvent of benzene and CH_2Cl_2 at room temperature yields a brown powder (compared to the green neutral cluster) that is not very crystalline, as indicated by the broad peaks in its pXRD pattern (Figure 9). ^{1}H NMR confirmed that the yellow filtrate of this reaction contains predominantly ferrocene. Of all the regular organic solvents tested, the brown powder was found to be soluble only in CH_3CN at room temperature and gave a dark brown solution, whereas the neutral $W_6S_8(PEt_2TTF)_6$ cluster dissolves to some extent in benzene and CH_2Cl_2 at room temperature, but not in CH_3CN. ^{1}H and ^{31}P NMR of the acetonitrile solution of this brown powder failed to give any signal over a wide range (a few hundred parts per million), presumably due to the paramagnetic broadening effect of the oxidized species.[60]

The IR spectra of the solid samples of the neutral $W_6S_8(PEt_2TTF)_6$ cluster and its oxidized product provided useful information on the identification of the latter (Figure 10). Two strong peaks at 839 and 559 cm^{-1} and a weak peak at 470 cm^{-1} in the spectra of the oxidized product are characteristic of the PF_6^- anion.[61] Bands arising from TTF (3060, 1523, 1248, 795, 740, and 645 cm^{-1})[62] as well as from ethylphosphine (2890−2990, 1466, 1408, 1378, 1042, 1030, 927, and 701 cm^{-1})[63] are present in both the neutral cluster and the oxidized product. McCarley et al. reported that the IR-allowed T_{1u} W−S stretching modes of the W_6S_8 unit in the molecular cluster gave a band at 378 cm^{-1}, which is characteristic of crystalline $W_6S_8L_6$ clusters.[64] A small peak at 379 cm^{-1} is observed in the far-IR spectrum of the neutral cluster, but in the far-IR spectrum of the less-crystalline oxidized product, only a broad band over the range of 370−385 cm^{-1} is seen. The loss of sharp W−S signal in amorphous materials has also been noted by McCarley et al. elsewhere.[65]

The XPS data of the neutral and oxidized $W_6S_8(PEt_2TTF)_6$ clusters and related compounds are summarized in Table 3. The tungsten binding energies at 30.9 eV ($4f_{7/2}$) and 33.0 eV ($4f_{5/2}$)[66] for both the neutral and oxidized complexes (Figure 11a) are characteristic of the W_6S_8 cluster units[19] and provide strong proof that the cluster core is retained in the oxidized product. The similar sulfur and phosphorus (ligand) binding energies in the neutral and oxidized clusters indicate similar coordination environments of these atoms in the two complexes, whereas extra phosphorus and fluorine peaks in the oxidized cluster correspond to PF_6 anion[67−69] (see Figure 11b for the phosphorus spectra).

We assign the composition of the oxidized cluster as $W_6S_8(PEt_2TTF)_6\cdot xPF_6$ on the basis of these characterization results. Elemental analysis on the oxidized powder[70] suggests $x \approx 5$. This composition may as well be justified through the powder pattern comparison of the neutral and oxidized compounds (Figure 9). The low-angle diffraction peaks in the oxidized product that are similar to those observed in neutral $W_6S_8(PEt_2TTF)_6\cdot 4C_6H_6$ suggest comparable cell dimensions. Similar dimensions might be expected, because the counteranion PF_6 can fit into the volume taken by solvent benzene molecules in the neutral compound, and benzene might be expected to be excluded from the more-ionic oxidized cluster complex.

Electrical Conductivity Measurements. Electrical conductivity measurements were performed on a pressed pellet of the oxidized powder. Several measurements were carried out on products from different batches, and a room-temperature conductivity in the range of $0.6-2.9 \times 10^{-4}$ S cm^{-1} was obtained. The conductivity was observed to decrease rapidly with decreasing temperature. The magnitude and temperature dependence of the conductivity suggest that $[W_6S_8(PEt_2TTF)_6]\cdot 5PF_6$ is still a semiconductor. A similar conductivity measurement was also performed on a pressed

(59) Setifi, F.; Ouahab, L.; Golhen, S.; Yoshida, Y.; Saito, G. *Inorg. Chem.* **2003**, *42*, 1791−1793.
(60) Mason, J., Ed. *Multinuclear NMR*; Plenum Press: New York, 1987.
(61) Kulczycki, A. *J. Phys. C: Solid State Phys.* **1981**, *14*, 2433−2439.
(62) Bozio, R.; Girlando, A.; Pecile, D. *Chem. Phys. Lett.* **1977**, *52*, 503−508.
(63) Green, J. H. S. *Spectrochim. Acta* **1968**, *24A*, 137−143.
(64) Zhang, X.; McCarley, R. E. *Inorg. Chem.* **1995**, *34*, 2678−2683.
(65) McCarley, R. E.; Hilsenbeck, S. J.; Xie, X. *J. Solid State Chem.* **1995**, *117*, 269−274.
(66) The 33.0 eV component in the oxidized cluster is slightly larger than that expected for W $4f_{5/2}$, indicating the presence of a small amount of another W oxidation state (W^{4+}); in our case, WS_2 is most likely. WS_2 may form from the decomposition of the cluster during either the oxidation reaction or XPS sample preparation. Therefore, the component at 33.0 eV is a mixture of W $4f_{5/2}$ (W_6S_8, major) and W $4f_{7/2}$ (WS_2, minor).
(67) Matsumoto, K.; Matsumoto, T.; Kawano, M.; Ohnuki, H.; Shichi, Y.; Nishide, T.; Sato, T. *J. Am. Chem. Soc.* **1996**, *118*, 3597−3609.
(68) Varughese, B.; Chellamma, S.; Lieberman, M. *Langmuir* **2002**, *18*, 7964−7970.
(69) Ohshita, T.; Tsukamoto, A.; Senna, M. *Phys. Status Solidi A* **2004**, *201*, 762−768.
(70) Anal. Calcd for $W_6S_{32}C_{60}H_{78}P_{11}F_{30}$ ($x = 5$): C, 18.77; H, 2.05; S, 26.73; F, 14.85; P, 8.87. Found: C, 20.25; H, 1.98; S, 24.36; F, 13.12; P, 7.84. Calcd molar ratios for $x = 5$: S/F, 1.07; F/P, 2.73. Found: S/F, 1.1; F/P, 2.73.

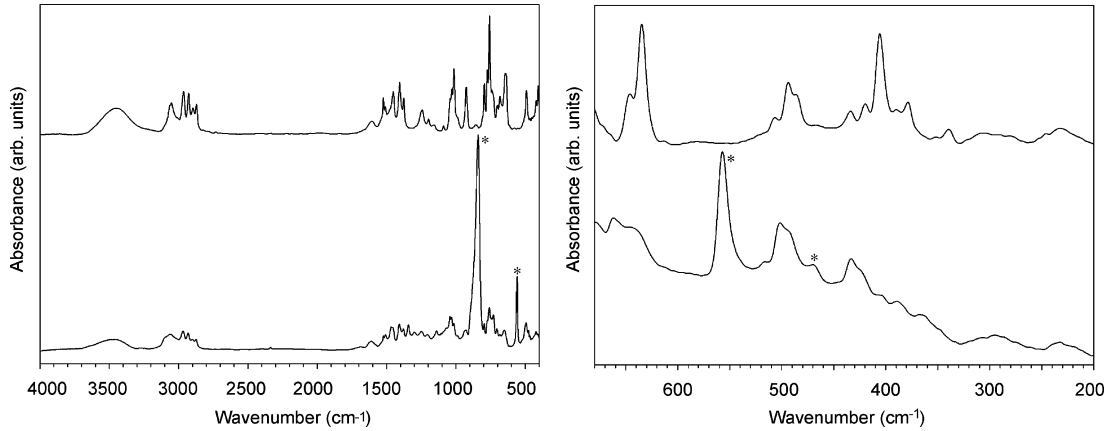

Figure 10. Mid-IR (left) and far-IR (right) spectra of the neutral $W_6S_8(PEt_2TTF)_6$ cluster (top) and its oxidized product (bottom). Peaks due to the PF_6^- anion are marked with asterisks.

Table 3. XPS Binding Energies (eV) for the Neutral and Oxidized Complexes and Related Compounds

	$W_6S_8(PEt_2TTF)_6$[a]	oxidized cluster[a]	$W_6S_8(PEt_3)_6$[b,17]	W_6S_8(pyridine)$_6$[b,19]	WS_2[b,19]
W $4f_{7/2}$	30.9	30.9	31.2	30.5	32.7
W $4f_{5/2}$	33.0	33.0[66]		32.6	34.8
S 2p (W_6S_8)	161.1, 162.2(sh)	161.1, 162.2(sh)	161.4, 162.2(sh)	160.6	162.4
S 2p (TTF)	163.6, 164.8(sh)	163.8, 165.0(sh)			
P 2p (bound ligand)	130.4, 131.3	130.6	130.8		
P 2p (PF_6)		136			
F 1s (PF_6)		685.9			

[a] Data calibrated with C 1s BE = 285 eV. [b] Literature data corrected to C 1s BE = 284.6 eV.

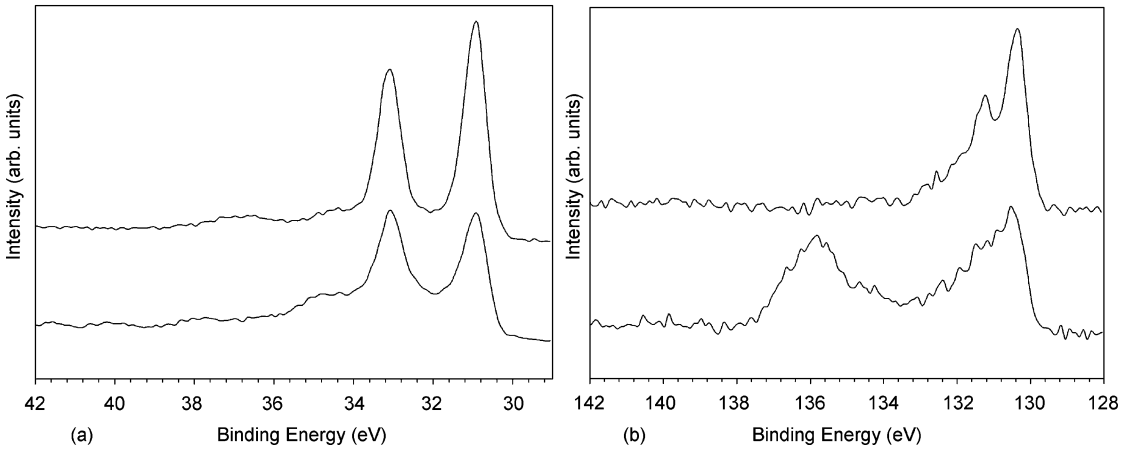

Figure 11. X-ray photoelectron of (a) W 4f and (b) P 2p spectra of the neutral $W_6S_8(PEt_2TTF)_6$ cluster (top) and its oxidized product (bottom). Binding energies were calibrated with C 1s BE = 285 eV.

pellet of the neutral $W_6S_8(PEt_2TTF)_6$ cluster. The resistance was too high to be measured by our apparatus, suggesting that $W_6S_8(PEt_2TTF)_6$ is an insulator. The partially oxidized cluster demonstrates improved electrical conductivity compared to the neutral species; however, better electrical performance should be expected from the fully oxidized product (with all six TTF ligands and the W_6S_8 core at the +1 oxidation state) or from an oxidized $W_6S_8(PEtTTF_2)_6$ cluster because of the larger number of TTF per cluster, as well as from a product with better crystallinity.

Increasing the TTF content in the cluster should promote intercluster TTF interactions in more than one dimension, thus it would be of interest to attach even more TTF-rich ligands such as $PTTF_3$ to the cluster. However, introduction of bulkier ligands causes solubility problems that hinder both crystallization and further oxidation of the system. It is therefore in large part the interplay of these two factors that defines our further experimental pursuits. With the well-established synthesis work on various TTF derivatives[71−73] as well as on other potentially interesting organic ligands,[74−77] we believe the reported work herein also opens up access to a wide variety of multifunctional molecular materials.

(71) Iyoda, M.; Kuwatani, Y.; Ueno, N.; Oda, M. *Chem. Commun.* **1992**, 158−159.
(72) Andreu, R.; Malfant, I.; Lacroix, P. G.; Cassoux, P. *Eur. J. Org. Chem.* **2000**, 737−741.
(73) Moore, A. J.; Batsanov, A. S.; Bryce, M. R.; Howard, J. A. K.; Khodorkovsky, V.; Shapiro, L.; Shames, A. *Eur. J. Org. Chem.* **2001**, 73−78.
(74) Yamashita, Y.; Saito, K.; Suzuki, T.; Kabuto, C.; Mukai, T.; Miyashi, T. *Angew. Chem., Int. Ed.* **1988**, *27*, 434−435.
(75) Wolmershäuser, G.; Johann, R. *Angew. Chem., Int. Ed.* **1989**, *28*, 920−921.
(76) Barclay, T. M.; Cordes, A. W.; Laat, R. H. d.; Goddard, J. D.; Haddon, R. C.; Jeter, D. Y.; Mawhinney, R. C.; Oakley, R. T.; Palstra, T. T. M.; Patenaude, G. W.; Reed, R. W.; Westwood, N. P. C. *J. Am. Chem. Soc.* **1997**, *119*, 2633−2641.
(77) Barclay, T. M.; Cordes, A. W.; Haddon, R. C.; Itkis, M. E.; Oakley, R. T.; Reed, R. W.; Zhang, H. *J. Am. Chem. Soc.* **1999**, *121*, 969−976.

Conclusions

In this paper, we reported the synthesis and characterization of a series of W_6S_8 molecular clusters attached to organic TTF derivative ligands. This is our first step in the pursuit of constructing multidimensional conductive networks. By combining the fascinating structural motifs of the high-symmetry inorganic octahedral cluster and $\pi-\pi$ stacking TTF molecules, we hope to build a network structure with good conductivity in two and even three dimensions upon oxidation.

Crystal structures of both mono-TTF- and bis-TTF-bound neutral clusters reveal intercluster interactions through TTF cofacial stacking in one and two dimensions, respectively. Electrochemical studies performed on cluster $W_6S_8(PEt_2TTF)_6$ show that both components (W_6S_8 and TTF) in these complexes are redox active and suggest the possibility of oxidizing them simultaneously.

Our chemical oxidation of $W_6S_8(PEt_2TTF)_6$ by $[Cp_2Fe]PF_6$ produced a powder product (chemical formula $[W_6S_8(PEt_2TTF)_6]\cdot 5PF_6$) with a room-temperature electrical conductivity of 1.77×10^{-4} S cm^{-1} on the basis of pressed pellet measurements.

Acknowledgment. This work was supported by National Science Foundation (NSF-CHE-0209934). We acknowledge Dr. Emil Lobkovsky for assistance with single-crystal X-ray diffraction experiments and Professors D. Venkataraman, Song Jin, and Barry Carpenter for useful discussions. We thank the Cornell High Energy Synchrotron Source (CHESS), which is supported by the National Science Foundation under Award DMR 0225180, for use of the Macromolecular Diffraction at the CHESS (MacCHESS) facility, which is supported by Award RR-01646 from the National Institutes of Health, through its National Center for Research Resources. M.Y. thanks Professor Fred Wudl for constructive e-mail discussions on cluster electrochemistry, Dr. Sandrine Perruchas for helpful discussions on TTF ligand synthesis and electrocrystallization techniques, Junliang Sun and Ji Feng for helping with the eH calculations, Dr. Josh Stapleton for performing the IR experiments, Mr. Bob Hengstebeck for performing the XPS measurements, Professor Geoffrey Coates for providing the HPLC facility, and Jeff Rose and Anna Cherian for helping with the HPLC experiments.

Supporting Information Available: Powder patterns of the cluster polymorphs. Cyclic voltammetry studies of the cluster/ligand extra reduction peak below 0 V. X-ray crystallographic files (CIF) for clusters **1**−**4**. This material is available free of charge via the Internet at http://pubs.acs.org.

CM0600071